HHS Public Access

Author manuscript

Nat Neurosci. Author manuscript; available in PMC 2018 September 19.

Published in final edited form as:

Nat Neurosci. 2018 May ; 21(5): 696–706. doi:10.1038/s41593-018-0121-5.

Myelin remodeling through experience-dependent oligodendrogenesis in the adult somatosensory cortex

E. G. Hughes[*,1,2,+], **J. L. Orthmann-Murphy**[1,3,*], **A. J. Langseth**[1], and **D. E. Bergles**[1,+]

[1]The Solomon H. Snyder Department of Neuroscience, Johns Hopkins University School of Medicine, Baltimore, MD

[2]Department of Cell and Developmental Biology, University of Colorado School of Medicine, Aurora, CO

[3]Department of Neurology, Johns Hopkins University School of Medicine, Baltimore, MD

Abstract

The generation of oligodendrocytes in the adult CNS provides a means to adapt the properties of circuits to changes in life experience. However, little is known about the dynamics of oligodendrocytes and the extent of myelin remodeling in the mature brain. Using longitudinal *in vivo* two photon imaging of oligodendrocytes and their progenitors in the mouse cerebral cortex, we show that myelination is an inefficient and extended process, with half of the final complement of oligodendrocytes generated after four months of age. Oligodendrocytes that successfully integrated formed novel sheaths on unmyelinated and sparsely myelinated axons, and were extremely stable, gradually changing the pattern of myelination. Sensory enrichment robustly increased oligodendrocyte integration, but did not change the length of existing sheaths. This experience-dependent enhancement of myelination in the mature cortex may accelerate information transfer in these circuits and strengthen the ability of axons to sustain activity by providing additional metabolic support.

Introduction

Axons throughout the CNS are ensheathed by myelin, a form of insulation that accelerates action potential propagation, and reduces both the energy expenditure required for transmission and the space necessary to assemble circuits capable of processing information with millisecond precision. The concentric layers of membrane that comprise myelin are

[+]Corresponding author: Correspondence to Dwight E. Bergles (dbergles@jhmi.edu) and Ethan G. Hughes (ethan.hughes@ucdenver.edu).

[*]Co-First Authors

Competing interests: The authors declare no competing financial interests.

Contributions: E.G.H. and D.E.B. conceived the project, designed the experiments, and wrote the manuscript with input from the other authors. J.O.M. and E.G.H. conducted the sensory manipulation experiments in Figs. 7,8 and analyzed data in Fig. 4. J.O.M contributed to the design of the sensory manipulation experiments, generated Supplementary Fig. 3, and contributed data to Fig. 1, Supplementary Figs. 4, 6, and 8. A.J.L. conducted and analyzed the viral labeling experiments for Fig. 5. E.G.H. executed and analyzed all other experiments described in the figures, text, and supplementary information.

formed by oligodendrocytes, each of which extend numerous processes to form discrete myelin internode segments along nearby axons. Oligodendrocytes have been studied intensively for decades, because of their important role in vertebrate evolution[1] and because their loss and failed regeneration contributes to debilitating diseases such as multiple sclerosis (MS). However, much of our knowledge about the behavior of oligodendrocytes and the process of myelination comes from studies of developmental myelination in white matter[2]. These pioneering studies indicate that most oligodendrocytes are generated early in life, that myelination is a constitutive process primarily induced by the presence of an axon of appropriate diameter, and that myelination continues until the axon surface is covered (with the exception of gaps, the nodes of Ranvier, between myelin segments), leading to populations of myelinated and unmyelinated axons that are maintained throughout life[3].

Recent studies suggest that interactions between oligodendrocytes and neurons are far more complex and less static than previously envisioned. It is now clear that oligodendrocytes also provide crucial metabolic support to axons[4,5], which are often far removed from their cell bodies and have limited access to the extracellular environment. In addition, although oligodendrocyte generation (oligodendrogenesis) and myelination begin during the perinatal period[2], oligodendrocyte precursor cells (OPCs) persist throughout life and support *de novo* formation of oligodendrocytes in the adult CNS in the absence of demyelinating pathology[6–10]. Increasing neuronal activity has been shown to enhance the generation of oligodendrocytes and thickness of individual myelin segments[11], suggesting that the same changes in activity that induce synaptic plasticity and alter neuronal excitability can also modify myelination. Changes in myelination within white matter tracks have been associated with motor learning in humans[12,13], and recent studies in mice showed that blocking the formation of new oligodendrocytes impairs motor learning[14,15], suggesting that the generation of new myelin segments is an important form of plasticity used to modify the properties of circuits in the CNS.

However, our knowledge about this form of plasticity remains incomplete, in part, because longitudinal studies of oligodendrocyte dynamics have not been performed in the intact CNS of adult mammals. Little is known about the extent to which oligodendrocytes and individual internode segments are remodeled in the adult brain and what types of experiences induce these changes. This is particularly true for cortical circuits, where many axons exhibit discontinuous myelination[16], providing abundant territory for addition of new myelin and greater potential for remodeling of existing sheaths.

Here, we performed longitudinal *in vivo* two photon imaging in the somatosensory cortex of adult transgenic mice in which oligodendrocytes and their individual myelin internodes can be resolved, to determine the extent of myelin dynamics in cortical gray matter. Our studies indicate that the period of oligodendrogenesis in the cerebral cortex is very prolonged, with more than half of oligodendrocytes in these circuits produced after four months of age. Although new oligodendrocytes were continually produced, their integration was highly inefficient, with a majority dying shortly after being generated. New myelin segments that appeared in the adult cortex were produced exclusively by newly generated oligodendrocytes, rather than by formation of new internodes from existing cells. Long-term imaging of individual myelin sheaths revealed that the majority were extraordinarily stable,

with only 1% changing in length over a period of seven weeks. Exposure of mice to sensory enrichment dramatically increased the frequency of new oligodendrocyte integration, but did not alter rate of sheath remodeling. Together, these results indicate that changes in life experience in adulthood alter the pattern of myelination in the cerebral cortex primarily through production of new oligodendrocytes, thereby providing an additional substrate for circuit plasticity in the adult brain.

Results

Oligodendrocyte generation continues in the adult cortex

Previous assessments of myelination changes in mammals involving histological analysis[2], genetic fate tracing[6–10] and *in vivo* magnetic resonance imaging (e.g. diffusion tensor imaging, DTI)[12,13], indicate that oligodendrogenesis and myelination also occurs in the adult CNS. Limitations of these approaches, particularly the restricted time and spatial resolution and inability to assess cell turnover, can be overcome through longitudinal *in vivo* fluorescence microscopy, as shown by the powerful insight obtained into the process of developmental myelination in the spinal cord of zebrafish[17,18]. To determine the extent of myelination changes in adult mammalian cortex, we obtained BAC transgenic mice in which EGFP is expressed under control of the promoter/enhancer for myelin-associated oligodendrocyte basic protein (Mobp) (*Mobp-EGFP* mice; Gensat[19,20]), a major component of myelin sheaths that is expressed late in oligodendrocyte maturation[21]. Immunocytochemical analysis of the somatosensory cortex revealed that all EGFP+ cells in this region co-localized with oligodendrocyte protein 2′,3′-cyclic-nucleotide 3′-phosphodiesterase (CNPase), but not the OPC-associated protein NG2 (Supplementary Fig. 1a–c), and all CNPase immunoreactive (CNP+) cells were also EGFP+, indicating that this mouse line allows detection of the full complement of oligodendrocytes (Supplementary Fig. 1d). *Mobp-EGFP* mice also allowed unambiguous visualization of individual internode segments along axons, with paranodal regions, defined by contactin-associated protein 1 (Caspr) immunoreactivity and proximity to voltage gated sodium channels, exhibiting enhanced fluorescence (Fig. 1a–c), presumably due to EGFP accumulation in paranodal loops. Using a label-free imaging technique that visualizes compact myelin (SCoRe, spectral confocal reflectance microscopy)[22], we found that EGFP+ internodes, but not paranodes, were detected with SCoRe (Fig. 1c), indicating that these EGFP+ internodes represent cytoplasmic channels surrounding compact myelin. In humans, the molecular layer of the cortex (layer I) is enriched with tangentially-oriented myelinated fibers that form the Plexus of Exner[23]. *In vivo* two photon imaging and volumetric analysis of the somatosensory cortex of *Mobp-EGFP* mice revealed that oligodendrocytes are similarly distributed throughout the upper layers of the murine cortex (Fig. 1d–g, Supplementary Movie 1).

To assess what proportion of oligodendrocytes are added in adult life, we performed volumetric *in vivo* two photon imaging in the somatosensory cortex of young adult (2–4 months), middle-aged (10–14 months), and aged (18–24 months) *Mobp-EGFP* mice. Although the relative distribution of oligodendrocytes in layers I–IV (0–400μm) of somatosensory cortex remained similar across ages, more than half of the oligodendrocytes present in middle-aged mice were produced after four months of age (Fig. 1d–g).

Oligodendrocyte density did not differ significantly between middle-aged and aged mice, indicating that the oligodendrocytes reach their zenith by middle-age (Fig. 1f). Although the density of oligodendrocytes varies by cortical depth (see Fig. 1g), we found that integration of new oligodendrocytes was uniform across cortical layers I–IV of somatosensory cortex (Supplementary Fig. 2), whereas neuron density remained constant over the 24 months examined (Supplementary Fig. 3). The density of OPCs also remained unchanged over this time period (Supplementary Fig. 3f), in accordance with the homeostatic behavior of these precusors[24]. The prolonged period of oligodendrogenesis in the murine cortex has important implications for studies of circuit plasticity and remyelination, as they are often performed during a period of intense myelination (2–4 months of age)[11,14,15,25,26].

Most oligodendrocytes generated in the adult brain fail to integrate

During perinatal development, 20–50% of newly formed oligodendrocytes undergo programmed cell death following differentiation[27,28]; however, the rate of successful integration of oligodendrocytes in the adult CNS has not been determined. To follow the differentiation of OPCs into mature oligodendrocytes *in vivo*, we generated triple transgenic mice (*Olig2-CreER;R26-lsl-tdTomato;NG2-mEGFP*) in which the entire oligodendrocyte lineage expressed tdTomato, but mEGFP was expressed only in OPCs (Fig. 2a–c, Supplementary Fig. 4); NG2 expression is rapidly downregulated when OPCs transform into oligodendrocytes, resulting in a loss of EGFP fluorescence[24], allowing us to monitor the generation and survival of newly generated oligodendrocytes by imaging of these two fluorophores. In middle-aged mice (8–14 months of age), OPCs (mEGFP+ tdTomato+) extended dynamic, radially oriented processes that were studded with motile filopodia (Supplementary Movies 2, 3). Upon differentiation, OPCs halted their migration and filopodial extension, and extended long, fine processes, characteristic of premyelinating oligodendrocytes (Fig. 2a–c; Supplementary Movies 2, 3). This morphological change was accompanied by a decrease in EGFP fluorescence and invasion of processes from neighboring OPCs into the territory of the differentiating cell, consistent with downregulation of repulsive cues[24] (Fig. 2d–f). Oligodendrocytes that successfully integrated into the cortex remained tdTomato+ throughout the duration of imaging (up to 40 days) (Fig. 2d; Supplementary Movie 2). However, many differentiating OPCs that lost EGFP fluorescence and displayed premyelinating oligodendrocyte morphology were present only transiently; within 1.8 ± 0.1 days of reducing mEGFP expression, they abruptly disappeared (35 cells; n = 3 mice, 8–14 months old). In rare cases, fragmentation of these cells was observed (Fig. 2f; Supplementary Movie 3), suggesting that they underwent programmed cell death. The death of newly formed oligodendrocytes was a rare event in the middle-aged cortex, occurring at a rate of 0.22 ± 0.08 events per day (n = 3 mice, 8–14 months old, imaged over 1.5 months), but the majority of OPCs that differentiated in the middle-aged cortex died at the premyelinating stage, with only 22% becoming stably integrated into these circuits (10/45 differentiating oligodendrocytes, n = 3 mice, 8–14 months old) (Fig. 2g). The death of premyelinating oligodendrocytes was distinct from the occasional turnover of OPCs, which was characterized by retraction of their processes and retention of both mEGFP and tdTomato until the cell disappeared (Supplementary Fig. 5). Although we were unable to track cells beyond about two months because of skull regrowth, the lack of oligodendrocyte death in *Mobp-EGFP* mice suggests that this minority of cells

becomes stably integrated. To determine if *in vivo* imaging may have decreased the viability of newly formed oligodendrocytes, we examined the proliferation of OPCs in longitudinally imaged *Olig2-CreER;R26-lsl-tdTomato;NG2-mEGFP* mice. OPCs homeostatically maintain their density[24], so phototoxicity-induced death of newly formed oligodendrocytes would be expected to enhance OPC proliferation. We found that OPC proliferation averaged 0.74 ± 0.09 events per day in *Olig2-CreER;R26-lsl-tdTomato;NG2-mEGFP* mice (n = 3 mice, 8–14 months old, tracked cells = 478) compared to 1.5 ± 0.1 events per day in *NG2-mEGFP* mice (n = 5 mice, 3–5 months old, tracked cells = 1118)[24], suggesting that the infrequent integration of newly formed oligodendrocytes does not reflect their increased sensitivity to longitudinal *in vivo* imaging.

Oligodendrogenesis supplements existing myelin in the mature brain

Previous studies have shown that some oligodendrocytes undergo apoptosis in the adult brain[29], suggesting that oligodendrogenesis may not just supplement existing myelin, but also replace oligodendrocytes lost through normal aging[9]. This scenario is attractive, as it provides an explanation for the persistence of OPCs throughout the CNS, which by remaining abundant and widely distributed. However, ^{14}C birth dating and recent genetic fate-mapping approaches suggests that most oligodendrocytes in the human brain have a long lifespan[7,30]. To determine whether adult oligodendrogenesis in the somatosensory cortex contributes to homeostatic maintenance of the oligodendrocyte population, we used *in vivo* two photon imaging to track individual oligodendrocytes in the cortex of middle-aged mice. Remarkably, every one of the approximately 600 oligodendrocytes monitored over this period was stable for a period of > 1.7 months (Fig. 3). A small number of new oligodendrocytes were generated over this time period, adding to the total population. These results indicate that there is minimal turnover of oligodendrocytes in the normal adult cortex, and that oligodendrogenesis continually expands the population of myelinating cells.

Discontinuous myelination persists in the adult brain

A recent study using serial EM reconstruction from an adult mouse (3–4 months) reported that many axons in layer II/III of the visual cortex exhibit discontinuous myelination, in which segments of myelin were often bordered by long stretches of axon devoid of myelin[16]. To determine if this phenomenon reflects an extended time course of myelination in the cortex (see Fig. 1) or a stable pattern of partial myelination, we compared the distribution of myelin internodes of layer I oligodendrocytes between young adult and middle-aged *Mobp-EGFP* mice. We classified all myelin sheaths in a 125 × 125 × 50 μm^3 area into three categories, Continuous, Interrupted, or Isolated; if the ends of the sheath were bordered by nodes of Ranvier on either side (abutting two other internodes), a sheath was classified as Continuous; if one side bordered a node of Ranvier and the other a bare segment of axon, it was classified as Interrupted; and if an internode was bordered by bare axon on either side, it was classified as Isolated (Fig. 4a–d). Isolated sheaths did not reflect short axons with only one myelin sheath, as they were found on axons that extended a significant distance within the imaging field (Fig. 4d). In both young and middle age mice, internodes in each of these categories were present in the somatosensory cortex (Fig. 4e,f), indicating that discontinuous myelination is not simply a feature of prolonged myelination. Despite the robust increase in density of myelin sheaths over this time period (Fig. 4g), the

relative proportion of internodes in each category was similar, although there was a trend towards more Continuous internodes in middle-aged mice (36% versus 47%, Young Adult: n = 5 mice; Middle-aged: n = 5 mice, p = 0.17, t(8) = −1.52, two-tailed Student's t-test; Fig. 4h). Moreover, the length of internodes, independent of category, was stable during this time (Fig. 4i). These results suggest that oligodendrocytes, once formed, establish defined domains along axons that do not require interactions with other myelin segments for stability.

Since the initial description oligodendrocytes, it has been postulated that there is heterogeneity within this glial cell type[31], a conclusion supported by recent single cell RNAseq analysis[32] and the existence of a sub-population of cortical oligodendrocytes with short, numerous myelin sheaths[33]. To determine whether oligodendrocytes vary in their production of different types of myelin sheaths (Continuous, Interrupted or Isolated), we labeled individual oligodendrocytes using an adeno-associated virus expressing EGFP under control of a fragment of the myelin basic protein (MBP) promoter (Fig. 5a,b). We found that oligodendrocytes in both young and middle-aged animals produced a similar number of myelin sheaths (Fig. 5c; Young Adult: 45 ± 4, n = 5 mice, 8 cells; Middle-aged: 43 ± 4, n = 5 mice, 8 cells, p = 0.62, t(14) = 0.51, two-tailed Student's t-test) and an equivalent proportion of Continuous, Interrupted, and Isolated sheaths (Fig. 5d; Young Adult: n = 5 mice, 8 cells; Middle-aged: n = 5 mice, 8 cells, Continuous, p = 0.99, t(14) = −0.005, Interrupted, p = 0.11, t(14) = 1.70, Isolated, p = 0.27, t(14) = −1.15, two-tailed Student's t-test). Moreover, myelin sheaths of oligodendrocytes in young and middle-aged animals were of similar length (Fig. 5e; Young Adult: n = 5 mice, 8 cells; Middle-aged: n = 5 mice, 8 cells, Continuous, p = 0.59, t(14) = 0.55, Interrupted, p = 0.52, t(14) = 0.65, Isolated, p = 0.73, t(14) = 0.36, two-tailed Student's t-test). These results indicate that oligodendrocytes adopt similar morphologies in the adult brain, despite being separated in generational time by ~ 8 months, suggesting that the constraints that limit target selection and internode length are conserved over this extended period of life.

Internode remodeling in the adult brain

Developmental studies indicate that the arrangement of internodes formed by each oligodendrocyte is established within a restricted time window after oligodendrocyte specification[34,35]. Although myelin sheath lengths decrease with aging[36,37] and adult-born oligodendrocytes have been shown to form shorter myelin sheaths[9], it is not known if oligodendrocytes have the capacity to remodel the length or position of internodes after this critical period. Such rearrangements would allow matching of sheath characteristics to changes in axon properties, such as rates of activity[17,18]. To determine if the length of existing myelin sheaths is altered in cortical circuits, we monitored individual myelin sheaths and nodes of Ranvier in the somatosensory cortex of young adult and middle-aged *Mobp-EGFP* mice *in vivo*. Stable integration of a new oligodendrocyte resulted in the concomitant appearance of new myelin sheaths in the vicinity of the cell body that gradually increased in length before stabilizing, often concluding with the formation of nodes of Ranvier (Fig. 6a; Supplementary Movie 4). In accordance with our internode analysis (see Fig. 4), oligodendrocytes also formed myelin segments along axons that were previously unmyelinated or sparsely myelinated, and these sheaths remained isolated for the duration of

the imaging period (up to three weeks; Supplementary Fig. 6). Thus, isolated internodes are not the net result of stranding, due to gradual removal of surrounding internodes, but rather the result of formation of new myelin sheaths along portions of axons that were previously devoid of myelin.

To define the extent of morphological reorganization of myelin sheaths in the middle-aged somatosensory cortex, we repeatedly imaged individual sheaths for 50 days. The majority of existing myelin sheaths and nodes of Ranvier remained constant in length and position throughout this time (Fig. 6b,c,d). However, a small fraction of myelin sheaths underwent retraction or extension (percentage of dynamic internodes: 0.97 ± 0.5%, n = 5 mice, 10–14 months old) (Fig. 6e,f; Supplementary Movies 5,6). Although it might be expected that isolated sheaths might have greater opportunity for length changes, dynamic myelin sheaths were equally represented across Continuous, Interrupted, and Isolated categories, and the average change in length (~15 μm) did not differ across these classifications (Fig. 6g; p = 0.58, one-way ANOVA). Hypertrophic EGFP+ CNPase+ processes that lacked MBP immunoreactivity (Supplementary Fig. 7), a morphology similar to the retracting sheaths detected through *in vivo* imaging, were also observed in *Mobp-EGFP* mice not subjected to cranial window surgery, suggesting that such events are not solely the result of experimental procedures associated with *in vivo* imaging. Together, these data indicate that the position and length of individual myelin sheaths are remarkably stable within cortical circuits.

Sensory enrichment enhances oligodendrogenesis and myelination in the adult brain

Studies in the developing prefrontal cortex have shown that social isolation leads to profound decreases in sheath number, sheath thickness, and myelin protein expression[25,26], indicating that changes in myelination can be induced independent of oligodendrogenesis. However, the extent to which different features of myelin are influenced by life experience in the adult cortex remains poorly understood. To determine if myelin sheath length remodeling is influenced by sensory experience in the somatosensory cortex, we monitored internode dynamics in middle-aged *Mobp-EGFP* mice that experienced enhanced sensory input, induced by housing mice in cages fitted with hanging strings of beads (Fig. 7a). Subjecting mice to this novel sensory experience has been shown to increase dendritic spine formation in the upper layers of somatosensory (barrel) cortex and promote long-lasting memory formation[38]. Repetitive time lapse imaging of internodes in this region revealed that exposure to this enhanced sensory experience did not alter the rate of extension or retraction of myelin sheaths, or influence the proportion of sheaths that were dynamic compared to control animals (Fig. 7). Thus, although changes in the length of individual sheaths occur at a low rate in the somatosensory cortex of naïve mice, this form of myelin reorganization is not strongly influenced by sensory experience.

Previous studies have shown that oligodendrogenesis can be increased in young adult animals (<1–3 months) by experimentally increasing neuronal activity or by altering social experience[11,25,26]. To determine whether changes in sensory experience modulate oligodendrogenesis in the middle-aged brain after the majority of myelination is complete, we compared new oligodendrocyte formation in the barrel cortex of *Mobp-EGFP* mice (10–14 months) housed in standard or sensory enriched cages (see Fig. 7a). Sensory enrichment

over a period of 20–22 days resulted in a five-fold increase in successfully integrated oligodendrocytes (primarily in layers II–III) (Fig. 8), expanding the total oligodendrocyte population by 1.1 ± 0.2% and resulting in the addition of approximately 250 new myelin sheaths (assuming that each oligodendrocyte generates approximately 50 myelin sheaths[39]) (Fig. 5c). This increase in myelin required whisker stimulation, as mice that that had their whiskers trimmed, but were housed in the same sensory-enriched environment, did not exhibit increases in oligodendrogenesis (Fig. 8c,d). Oligodendrocytes generated as a result of sensory enrichment remained in the cortex for an additional three weeks after the mice were returned to standard housing conditions (Supplementary Fig. 8), indicating that these cells became stably integrated into cortical circuits. Together, these data reveal that sensory experience in adult life modifies the pattern of myelination in the somatosensory cortex by altering the production of oligodendrocytes.

Discussion

The cerebral cortex plays a crucial role in processing sensory information and enabling higher cognitive ability. Although classically defined as a gray matter region, some axons that reside in the cortex become ensheathed with myelin, a phenomenon that coincides with the maturation of functional properties[2]. However, even in the adult brain, many axons in the cortex remain unmyelinated or partially myelinated[16] providing abundant territory for the formation of new myelin sheaths. Recent studies indicate that oligodendrocytes continue to be generated in the cortex into adulthood[2,6–10], and that key features of myelin, including the thickness and length of sheaths can be modified by neuronal activity[11,25,26], suggesting that formation of new myelin sheaths, and remodeling of existing sheaths, may represent additional forms of activity-dependent plasticity used to adapt the properties of cortical circuits to life experience. However, much of our knowledge about myelin plasticity comes from studies in white matter and early stages of life, or has been inferred from indirect measures of myelination. Much less is known about the dynamics of oligodendrocytes and myelin sheaths in mature cortical circuits under physiological conditions. Our studies indicate that oligodendrocyte formation continues over a very extended time course in the cortex, with oligodendrocytes doubling in number from 4 to 10 months of age. The generation of oligodendrocytes was highly inefficient, with less than one quarter of differentiation events leading to stable integration. However, oligodendrocytes that became integrated were remarkably stable, with no turnover observed over a period of almost two months. Although there are many potential means of modifying myelin, few sheaths changed their length or were removed over this time period, and the degree of remodeling that was observed was not modified by sensory experience. In contrast, oligodendrogenesis was profoundly increased when animals were exposed to enhanced sensory experience, resulting in the formation of hundreds of new myelin sheaths in barrel cortex. This ability to change the pattern of myelination in the somatosensory cortex by producing new oligodendrocytes provides an additional substrate for modifying the processing capabilities of mature cortical circuits in response to life experience.

The process of developmental myelination in the CNS is inefficient, characterized by apoptotic death of many oligodendrocytes during the premyelinating stage[27,28], suggesting that there is a critical time window for integration and that the threshold for integration is

high. Our studies indicate that although OPCs continue to differentiate in the adult brain, the barriers to full maturation and integration in these mature circuits remain high, with only a small fraction of these differentiation events leading to the formation of new myelin sheaths (Fig. 2). This inefficient process can be tolerated without jeopardizing future myelination, because it does not ultimately deplete the brain of progenitors[24]. Recent studies indicate that interneurons in the spinal cord prevent their myelination through expression of Junctional Adhesion Molecule 2 (JAM2)[40]. Although there are likely many factors that influence oligodendrocyte survival, the expression of similar inhibitory cues by cortical axons could restrict the ability of nascent sheaths to proceed past developmental checkpoints within a critical time window after differentiation has been initiated.

Once differentiating OPCs were successfully integrated as oligodendrocytes, they were highly stable in the adult cortex. We failed to observe loss of a single oligodendrocyte using longitudinal *in vivo* imaging in middle-aged mice over 50 days (Fig. 3) and adult-born oligodendrocytes that became stably integrated were observed up to 40 days following initial integration (Fig. 2g, Supplementary Fig. 8b). These data are consistent with recent findings using ^{14}C carbon-dating in humans showing that oligodendrocytes are largely stable throughout life[7], and a genetic fate-mapping study in mice that suggests that adult-born oligodendrocytes in the murine brain have a half-life of over 10 years[30].

Living imaging studies in developing zebrafish have shown that new oligodendrocytes generate their myelin sheaths within five hours and remain stable for 2–3 weeks[34]. However, whether existing myelin sheaths of mature oligodendrocytes retain the capacity for remodeling remains unclear. Young et al. reported that adult-born oligodendrocytes in the completely myelinated optic nerve produce more numerous and shorter internodes than oligodendrocytes formed during early development[9], suggesting that pre-existing myelin can be remodeled to accommodate newly formed myelin sheaths. Our *in vivo* longitudinal studies of individual myelin sheaths in the adult somatosensory cortex indicate that existing myelin sheaths rarely change their length (Fig. 6), perhaps because of the extensive unmyelinated regions available.

Our distribution analysis of individual myelin sheaths in the middle-aged brain indicate that discontinuous myelination is sustained in animals up to one year of age (Fig. 4), indicating that it does not reflect an early developmental process. Reconstruction of individual oligodendrocytes revealed that each provides sheaths that can be isolated or part of a larger myelinated segment made up of multiple internodes, suggesting that these sheaths do not arise from cell autonomous differences among oligodendrocytes (Fig. 5). Time lapse imaging further revealed that newly generated oligodendrocytes formed isolated sheaths on previously unmyelinated axons (Supplementary Fig. 6), indicating that these sheaths do not become isolated through removal/retraction of neighboring sheaths, although sheath retraction was occasionally observed (Fig. 6).

The function of discontinuous myelination in the cortex remains uncertain. Isolated sheaths may still enable oligodendrocytes to provide metabolic support to axons[4,5], although the ability of surrounding unmyelinated regions to access the extracellular environment would seem to reduce the necessity for transfer of energy substrates such as lactate from

oligodendrocytes. Subtle differences in action potential conduction and membrane excitability induced by these sheaths may create sufficient timing differences to alter the processing of information in cortical circuits. Future studies in which myelination can be selectively disrupted within defined circuits will help test these possibilities.

The doubling of oligodendrocyte number from young adulthood to middle-age that we observed in the somatosensory cortex (Fig. 1) is consistent with ^{14}C carbon-dating in humans, which indicate that the number of oligodendrocytes in the cortex does not plateau until the fourth decade of life[7]. Many studies of cortical function and plasticity, as well as the recovery from demyelination, have been performed at an age when myelination patterns are immature, which may increase their ability to contribute to plasticity[14,15]. Our longitudinal studies of oligodendrogenesis and internode dynamics revealed that sensory enrichment enhanced myelination by stimulating the production of new oligodendrocytes, rather than inducing the formation of new sheaths by existing oligodendrocytes (Fig. 8). The eventual reduction in ability to produce new oligodendrocytes in the aged brain, whether through a decrease in suitable substrates (i.e. axons with a low threshold for myelination) or through aging-related decline in the ability of OPCs to undergo differentiation[41] may contribute to the decline in cognitive ability with age[37].

Our analysis of oligodendrocytes focused exclusively on layers I-IV due to limitations in the ability to resolve structures at great depth using two photon imaging of EGFP. It is possible that oligodendrocyte behavior may differ between gray and white matter regions in the adult CNS, and between these regions and deeper layers of the cortex. Indeed, the kinetics of oligodendrocyte generation differs between gray and white matter[6–8], and it has been proposed that the prolonged period of oligodendrocyte generation and sparse myelination of the cortex may have a role in higher brain function[7]. Application of new approaches for deep brain, high-resolution imaging[42] of regions such as the corpus callosum will be necessary to define oligodendrocyte and myelin sheath dynamics in adult white matter.

Our data indicate that sensory experience modifies the integration of new oligodendrocytes, but does not induce existing oligodendrocytes to form new sheaths or alter the length of their sheaths (Figs. 7,8). However, it is possible that other structural and functional aspects of myelin not assessed here, such as sheath thickness[11,25,26] or metabolic support[4,5], could be modified in this context, or that sheath remodeling occurs with a delay of many weeks after sensory enrichment. As we learn more about the identity of myelinated axons in the cerebral cortex[43], we will be able to assess how discrete patterns of activity influence the structure and stability of myelin, and the contributions of these changes to cortical function and behavior.

Analysis of demyelinated areas in brain tissue from human MS patients revealed a high incidence of oligodendrocytes with a premyelinating morphology[44], suggesting that the process of oligodendrocyte maturation may be stalled. Our time lapse imaging of OPC maturation in the cortex (Fig. 2) indicate that this premyelinating stage is normally fleeting, and cells that do not integrate undergo apoptosis and are rapidly removed. Although the premyelinating stage may be stabilized in the lesion environment, it is also possible that the presence of premyelinating cells reflects continuous oligodendrogenesis due to failed

integration. Identification of factors that promote this later stage of maturation, or that lower barriers to integration, may work synergistically with agents that promote the differentiation of OPCs[45] to further enhance remyelination and lesion repair and promote functional recovery in disease and injury contexts.

Methods

Animals

Both female and male mice were used for experiments and were randomly assigned to experimental groups. All mice were healthy and did not display any obvert behavioral phenotypes, and no animals were excluded from the analysis. Generation and genotyping of BAC transgenic lines *Mobp-EGFP*[19] (Gensat), *NG2-mEGFP*[24], *Olig2-CreER*[46], and tdTomato reporter mouse line[47] (Ai14, Allen Brain Institute) have been previously described. For experiments using the inducible Cre-loxP system to label oligodendrocyte lineage cells, mice were injected with tamoxifen (see Tamoxifen injection section below for details). Mice were maintained on a 12 hr. light/dark cycle, housed in groups no larger than 5 and food and water were provided *ab libitum*. All animal experiments were performed in strict accordance with protocols approved by the Animal Care and Use Committee at Johns Hopkins University.

In vivo two photon microscopy

Cranial windows were prepared as previously described[24]. Briefly, mice (2–24 months old) were anesthetized with isoflurane (induction, 5%; maintenance, 1.5% – 2.0%, mixed with 0.5 l/min O_2) and their body temperature was maintained at 37°C with a thermostat-controlled heating plate. The skin over the right cerebral hemisphere was removed and the skull cleaned. A 2 ×2 mm region of skull over somatosensory cortex (−0.5 to −2 mm post bregma and 1 to 3.5 mm lateral) was either thinned (~20 μm thickness) or removed using a high-speed dental drill. For cranial windows, a piece of cover glass (VWR, No. 1) was placed in the craniotomy and sealed with dental cement (C&B Metabond) and a custom metal plate with a central hole was attached to the skull for head stabilization. *In vivo* imaging sessions began immediately after surgery (thinned-skull preparation) or after a minimum of three weeks (chronic cranial window), as noted in the text. During imaging sessions, mice were anesthetized with isoflurane and immobilized by attaching the head plate to a custom stage. Images were collected using a Zeiss LSM 710 microscope equipped with a GaAsP detector using a mode- locked Ti:sapphire laser (Coherent Ultra) tuned to 920 nm. The average power at the sample during imaging was <30 mW. Vascular landmarks were used to identify the same cortical area over longitudinal imaging sessions. Image stacks were either 425 μm × 425 μm × 100 μm (2048 × 2048 pixels; corresponding to cortical layer I) or 425 μm × 425 μm × 500 μm (1024 × 1024 pixels; corresponding to layers I – IV) from the cortical surface.

Viral Injections

Injection of adeno-associated virus into adult mouse sensory cortex was performed according to standard protocols. Briefly, mice 11–13 weeks old (young cohort) or 52–60 weeks old (middle-aged cohort) were anesthetized using Isoflurane (Baxter). Animals were

head mounted in an Angle Two Stereotaxic Instrument (Leica Biosystems) and a micro-drill (Ideal) was used to make a burr hole through the skull. The injection was targeted to sensory cortex at 1.0 mm posterior to Bregma, 3.0 mm lateral, and 100 nm depth into the cortex. 1×10^9 viral genomes of AAV9-MBP-eGFP (kind gift from Dr. Thomas McCown, UNC) were injected using a Nanoject (Drummond Scientific) at 23 nL per second. At least 21 days after the injection, animals were perfused and tissue was collected for immunohistochemistry.

Immunohistochemistry

Mice were deeply anesthetized with sodium pentobarbital (100 mg/kg b.w.) and perfused transcardially with 4% paraformaldehyde (PFA in 0.1 M phosphate buffer [pH 7.4]). For horizontal sections, cortices were flat-mounted between glass slides and post fixed in 4% PFA overnight at 4°C, transferred to 30% sucrose solution (in PBS [pH 7.4]), and stored at 4°C for more than 48 hr. Brains were extracted frozen in TissueTek, sectioned (coronal, bregma 0.2 to −1.9 mm; horizontal, 0 – 1 mm) at 30 – 50 μm thick. Immunofluorescence was performed on free-floating sections. Sections were preincubated in blocking solution (5% normal donkey serum, 0.3% Triton X-100 in PBS [pH 7.4]) for 1 or 2 hr at room temperature, then incubated for 2 days at 4°C in primary (listed along with secondary antibodies in Supplementary Table 1). Secondary antibody incubation was performed at room temperature for 2–4 hr. Sections were mounted on slides with ProLong anti-fade reagent (Invitrogen). Images were acquired using either an epifluorescence microscope (Zeiss Axio-imager M1) with Axiovision software (Zeiss) or a confocal laser-scanning microscope (Zeiss LSM 510 Meta; Zeiss LSM 710).

Sensory enrichment

For sensory enrichment, mice were placed in standard mouse cages containing a grid of strings of beads spaced 1.5 to 3 cm apart and a tolerance of 1 cm positional movement for 3 weeks over both light and dark cycles[38]. For sensory deprivation, left-side whiskers were completely removed every 2–3 days for three weeks. Mice were anesthetized with isoflurane for whisker removal (or mock whisker removal with anesthesia for control). The same baseline region of contralateral somatosensory barrel cortex was re-imaged after three weeks for either control (standard cage +/− isoflurane exposure every 2–3 days), sensory enrichment, sensory deprivation, or a combination of sensory deprivation and enrichment conditions.

Image processing and analysis

Image stacks and time series were analyzed using FIJI/ImageJ. All analysis was performed on unprocessed images except for middle-aged myelin sheath analysis images. For presentation in figures, image brightness and contrast levels were adjusted for clarity. Myelin sheath images were additionally processed with a Mean filter (radius = 2 pixels) to de-noise. For the pseudo-color display of individual myelin sheaths (Figs. 6,7), a three-dimensional region of interest was defined for each time point and a custom-written FIJI script was used to segment and/or colorize the sheath. Longitudinal image stacks were registered using FIJI plugins ‘Correct 3D drift’[48] or ‘PoorMan3DReg’ and then randomized for analysis by a blinded observer.

Cell tracking

Cells were followed in three dimensions using custom FIJI scripts by defining EGFP+ cell bodies at each time point, recording *xyz* coordinates, and defining cellular behavior (new, dying, proliferating, differentiating, or stable cells). OPC migration, proliferation, death, and differentiation were defined as previously described[24]. Briefly, OPCs were classified as proliferating if two cells appeared in the same location and cell bodies were separated by less than 50 μm. Dying OPCs displayed a shortening and blebbing of processes and a complete disappearance of EGFP (*NG2-mEGFP*) and tdTomato (*Olig2-CreER;R26-lsl-tdTomato*) fluorescence simultaneously (Supplementary Fig. 4). Differentiating OPCs exhibited morphological changes classically associated with oligodendrocyte differentiation, including a progressive decrease in EGFP (*NG2-mEGFP*) fluorescence and sustained tdTomato (*Olig2-CreER;R26-lsl-tdTomato*) fluorescence (Fig. 2). Differentiating OPCs that died prior to integrating as mature oligodendrocytes lost EGFP fluorescence, had radial, highly branched processes characteristic of premyelinating oligodendrocytes, and abruptly lost tdTomato fluorescence. TdTomato+ cell fragments were occasionally observed in the vicinity of the original cell (Fig. 2e,f).

Myelin sheath analysis

In vivo Z-stacks collected from *Mobp-EGFP* mice were acquired using two photon microscopy. Z-stacks from middle-aged mice were background subtracted and processed with a 0.5 – 1 pixel median filter to aid in the identification of myelin internodes. All myelin sheaths that terminated within an area of 125 × 125 × 50 μm^3 from the pial surface were traced in FIJI using Simple Neurite Tracer[49] and identified as Continuous, Interrupted, Isolated. Continuous sheaths have nodes of Ranvier on either side (abutting two other sheaths). Interrupted sheaths are bordered by only one node of Ranvier, the other end of the sheath extending along a bare segment of axon. Isolated sheaths are bordered by bare axon on either side. Myelin sheaths within the field that extended beyond the imaged area or could not be definitively identified were classified as ‘undefined’. Myelin paranodes were identified by increased EGFP fluorescence intensity (see Fig. 1). Nodes of Ranvier were identified by plotting an intensity profile across the putative node; if the intensity decreased to zero between the adjacent oligodendrocyte processes, and the length of the gap between EGFP+ processes was <5 μm, the structure was considered a node[50]. For each field, myelin sheaths were traced by one investigator and independently assessed by a second investigator.

Myelin sheath analysis of individual oligodendrocytes

Confocal Z-stacks of virally infected, EGFP+ oligodendrocytes were acquired at 40x, oil immersion, objective on a Zeiss 510 microscope. Myelin sheaths were traced in Imaris (Bitplane) to quantify the number of myelin sheaths per oligodendrocyte and to categorize each myelin sheath as Isolated (no adjacent myelin sheaths), Interrupted (one adjacent myelin sheath), Continuous (two adjacent myelin sheaths), or Undefined (cut by the sectioning plane so that adjacent myelin sheaths could not be determined). The length of each myelin sheath was also quantified. Because isolated GFP-positive oligodendrocytes were chosen for this analysis, all GFP-positive myelin sheaths within close proximity (~50

μm) to a GFP-positive oligodendrocyte cell body were considered connected to that oligodendrocyte.

Tamoxifen injections

Tamoxifen (Sigma; T5648-1G; CAS:10540-29-1) was weighed and dispersed in sunflower seed oil (Sigma; S5007; CAS: 8001-21-6) for a final concentration of 10mg/ml. The solution was vortexed vigorously and then sonicated for five minutes. This cycle was repeated three-to-four times until tamoxifen was completely dissolved. The tamoxifen/oil emulsion was stored at 4°C protected from light and used for maximum of seven days. Mice four weeks-old were injected intraperitoneally with 100mg/kg body weight of the tamoxifen/oil emulsion once a day for five consecutive days to induce Cre recombination.

Statistics and Reproducibility

No statistical methods were used to pre-determine sample sizes but our sample sizes are similar to those reported in previous publications. Data analysis was performed blind to the conditions of the experiments. Statistical analyses were performed with Origin Pro (OriginLab) or Excel (Microsoft). All datasets were tested with the Shapiro-Wilk test to determine normality. Significance was determined using unpaired two-tailed Student's t-test or one-way ANOVA with Tukey *post hoc* test. Each figure legend contains the statistical tests used to measure significance and the corresponding significance level (p value). N represents the number of animals used in each experiment. Data are reported as mean ± SEM and $p < 0.05$ was considered statistically significant. Additional details can be found in the Supplementary Methods Checklist.

Data availability

All data that support the findings, tools, and reagents will be shared on an unrestricted basis; requests should be directed to the corresponding authors.

Code availability

All published code will be shared on an unrestricted basis; requests should be directed to the corresponding authors.

Antibody validation

Antibody source, dilution, catalog number, and unique identifier are listed in Supplementary Table 2. Antibodies were selected according to the antibody validation profiles reported by the distributing companies and in publications. Noncommercial antibodies (anti-Caspr and anti-NG2 antibodies) were selected according to validation profiles reported in publications and are specifically referenced by the citation and PMID.

Life Sciences Reporting Summary

Mouse lines used in this study are listed in Supplementary Table 1. Age of the experimental animals are listed in corresponding figure legends. Further information on experimental design is available in the Life Sciences Reporting Summary.

Supplementary Material

Refer to Web version on PubMed Central for supplementary material.

Acknowledgments

We thank M. Pucak, N. Ye, H. Hsieh, and A. Doreswamy for technical assistance, T. Shelly for machining expertise, and members of the Bergles laboratory for discussions. We thank Dr. Thomas McCown for the kind gift of AAV9-MBP-eGFP virus. E.G.H was supported by a NRSA grant from the NIH (F32NS076098), the Boettcher Foundation, the Whitehall Foundation, the Conrad N. Hilton Foundation (17324), and the National Multiple Sclerosis Society (RG-1701-26733). J.O.M. was supported by a National Multiple Sclerosis Society Postdoctoral Fellowship (FG 2092-A-1) and the Conrad N. Hilton Foundation (17314). A.J.L. was supported by a National Multiple Sclerosis Society Postdoctoral Fellowship (FG 20114-A-1). Funding was provided by grants from the NIH (NS051509, NS050274), the Dr. Miriam and Sheldon G. Adelson Medical Research Foundation, the Brain Science Institute at Johns Hopkins University and the Johns Hopkins Medicine Discovery Fund to D.E.B.

References

1. Nave KA. Myelination and support of axonal integrity by glia. Nature. 2010; 468:244–252. [PubMed: 21068833]
2. Yakovlev, P., Lecours, A. The myelogenetic cycles of regional maturation of the brain. In: Minkowski, A., editor. Regional development of the brain in early life. Vol. 1967. Oxford: Blackwell Scientific Publications; 1967.
3. Baumann N, Pham-Dinh D. Biology of Oligodendrocyte and Myelin in the Mammalian Central Nervous System. Physiol Rev. 2001; 81:871–927. [PubMed: 11274346]
4. Fünfschilling U, et al. Glycolytic oligodendrocytes maintain myelin and long-term axonal integrity. Nature. 2012; 485:517–521. [PubMed: 22622581]
5. Lee Y, et al. Oligodendroglia metabolically support axons and contribute to neurodegeneration. Nature. 2012; 487:443–448. [PubMed: 22801498]
6. Kang SH, Fukaya M, Yang JK, Rothstein JD, Bergles DE. NG2+ CNS Glial Progenitors Remain Committed to the Oligodendrocyte Lineage in Postnatal Life and following Neurodegeneration. Neuron. 2010; 68:668–681. [PubMed: 21092857]
7. Yeung MSY, et al. Dynamics of Oligodendrocyte Generation and Myelination in the Human Brain. Cell. 2014; 159:766–774. [PubMed: 25417154]
8. Rivers LE, et al. PDGFRA/NG2 glia generate myelinating oligodendrocytes and piriform projection neurons in adult mice. Nat Neurosci. 2008; 11:1392–1401. [PubMed: 18849983]
9. Young KM, et al. Oligodendrocyte Dynamics in the Healthy Adult CNS: Evidence for Myelin Remodeling. Neuron. 2013; 77:873–885. [PubMed: 23473318]
10. Dimou L, Simon C, Kirchhoff F, Takebayashi H, Götz M. Progeny of Olig2-Expressing Progenitors in the Gray and White Matter of the Adult Mouse Cerebral Cortex. J Neurosci. 2008; 28:10434–10442. [PubMed: 18842903]
11. Gibson EM, et al. Neuronal Activity Promotes Oligodendrogenesis and Adaptive Myelination in the Mammalian Brain. Science. 2014; 344:1252304. [PubMed: 24727982]
12. Scholz J, Klein MC, Behrens TEJ, Johansen-Berg H. Training induces changes in white-matter architecture. Nat Neurosci. 2009; 12:1370–1371. [PubMed: 19820707]
13. Bengtsson SL, et al. Extensive piano practicing has regionally specific effects on white matter development. Nat Neurosci. 2005; 8:1148–1150. [PubMed: 16116456]
14. McKenzie IA, et al. Motor skill learning requires active central myelination. Science. 2014; 346:318–322. [PubMed: 25324381]
15. Xiao L, et al. Rapid production of new oligodendrocytes is required in the earliest stages of motor-skill learning. Nat Neurosci. 2016; 19:1210–1217. [PubMed: 27455109]
16. Tomassy GS, et al. Distinct Profiles of Myelin Distribution Along Single Axons of Pyramidal Neurons in the Neocortex. Science. 2014; 344:319–324. [PubMed: 24744380]

17. Mensch S, et al. Synaptic vesicle release regulates myelin sheath number of individual oligodendrocytes in vivo. Nat Neurosci. 2015; 18:628–630. [PubMed: 25849985]
18. Hines JH, Ravanelli AM, Schwindt R, Scott EK, Appel B. Neuronal activity biases axon selection for myelination in vivo. Nat Neurosci. 2015; 18:683–689. [PubMed: 25849987]
19. Gong S, et al. A gene expression atlas of the central nervous system based on bacterial artificial chromosomes. Nature. 2003; 425:917–925. [PubMed: 14586460]
20. Kang SH, et al. Degeneration and impaired regeneration of gray matter oligodendrocytes in amyotrophic lateral sclerosis. Nat Neurosci. 2013; 16:571–579. [PubMed: 23542689]
21. Holz A, et al. Molecular and developmental characterization of novel cDNAs of the myelin-associated/oligodendrocytic basic protein. J Neurosci. 1996; 16:467–477. [PubMed: 8551331]
22. Schain AJ, Hill RA, Grutzendler J. Label-free in vivo imaging of myelinated axons in health and disease with spectral confocal reflectance microscopy. Nat Med. 2014; 20:443–449. [PubMed: 24681598]
23. Exner, S. Untersuchungen über die Localisation der Functionen in der Grosshirnrinde des Menschen. Wien: Braumüller; 1881.
24. Hughes EG, Kang SH, Fukaya M, Bergles DE. Oligodendrocyte progenitors balance growth with self-repulsion to achieve homeostasis in the adult brain. Nat Neurosci. 2013; 16:668–676. [PubMed: 23624515]
25. Makinodan M, Rosen KM, Ito S, Corfas G. A Critical Period for Social Experience–Dependent Oligodendrocyte Maturation and Myelination. Science. 2012; 337:1357–1360. [PubMed: 22984073]
26. Liu J, et al. Impaired adult myelination in the prefrontal cortex of socially isolated mice. Nat Neurosci. 2012; 15:1621–1623. [PubMed: 23143512]
27. Barres BA, et al. Cell death and control of cell survival in the oligodendrocyte lineage. Cell. 1992; 70:31–46. [PubMed: 1623522]
28. Trapp BD, Nishiyama A, Cheng D, Macklin W. Differentiation and Death of Premyelinating Oligodendrocytes in Developing Rodent Brain. J Cell Biol. 1997; 137:459–468. [PubMed: 9128255]
29. Cerghet M, et al. Proliferation and Death of Oligodendrocytes and Myelin Proteins Are Differentially Regulated in Male and Female Rodents. J Neurosci. 2006; 26:1439–1447. [PubMed: 16452667]
30. Tripathi RB, et al. Remarkable Stability of Myelinating Oligodendrocytes in Mice. Cell Rep. 2017; 21:316–323. [PubMed: 29020619]
31. del Rio Hortega P. Estudio sobre la neuroglia. Glia Escasas Ramificaciones Oligodendroglia Bol Real Soc Espan Biol. 1921; 9:69–120.
32. Marques S, et al. Oligodendrocyte heterogeneity in the mouse juvenile and adult central nervous system. Science. 2016; 352:1326–1329. [PubMed: 27284195]
33. Murtie JC, Macklin WB, Corfas G. Morphometric analysis of oligodendrocytes in the adult mouse frontal cortex. J Neurosci Res. 2007; 85:2080–2086. [PubMed: 17492793]
34. Czopka T, ffrench-Constant C, Lyons DA. Individual Oligodendrocytes Have Only a Few Hours in which to Generate New Myelin Sheaths In Vivo. Dev Cell. 2013; 25:599–609. [PubMed: 23806617]
35. Watkins TA, Emery B, Mulinyawe S, Barres BA. Distinct Stages of Myelination Regulated by γ-Secretase and Astrocytes in a Rapidly Myelinating CNS Coculture System. Neuron. 2008; 60:555–569. [PubMed: 19038214]
36. Lasiene J, Matsui A, Sawa Y, Wong F, Horner PJ. Age-related myelin dynamics revealed by increased oligodendrogenesis and short internodes. Aging Cell. 2009; 8:201–213. [PubMed: 19338498]
37. Peters A, Kemper T. A review of the structural alterations in the cerebral hemispheres of the aging rhesus monkey. Neurobiol Aging. 2012; 33:2357–2372. [PubMed: 22192242]
38. Yang G, Pan F, Gan WB. Stably maintained dendritic spines are associated with lifelong memories. Nature. 2009; 462:920–924. [PubMed: 19946265]

39. Chong SYC, et al. Neurite outgrowth inhibitor Nogo-A establishes spatial segregation and extent of oligodendrocyte myelination. Proc Natl Acad Sci. 2012; 109:1299–1304. [PubMed: 22160722]
40. Redmond SA, et al. Somatodendritic Expression of JAM2 Inhibits Oligodendrocyte Myelination. Neuron.
41. Shen S, et al. Age-dependent epigenetic control of differentiation inhibitors is critical for remyelination efficiency. Nat Neurosci. 2008; 11:1024–1034. [PubMed: 19160500]
42. Ouzounov DG, et al. In vivo three-photon imaging of activity of GCaMP6-labeled neurons deep in intact mouse brain. Nat Methods. 2017; 14:388–390. [PubMed: 28218900]
43. Micheva KD, et al. A large fraction of neocortical myelin ensheathes axons of local inhibitory neurons. eLife. 2016; 5:e15784. [PubMed: 27383052]
44. Chang A, Tourtellotte WW, Rudick R, Trapp BD. Premyelinating Oligodendrocytes in Chronic Lesions of Multiple Sclerosis. N Engl J Med. 2002; 346:165–173. [PubMed: 11796850]
45. Green AJ, et al. Clemastine fumarate as a remyelinating therapy for multiple sclerosis (ReBUILD): a randomised, controlled, double-blind, crossover trial. The Lancet. 2017; 0
46. Takebayashi H, et al. The Basic Helix-Loop-Helix Factor Olig2 Is Essential for the Development of Motoneuron and Oligodendrocyte Lineages. Curr Biol. 2002; 12:1157–1163. [PubMed: 12121626]
47. Madisen L, et al. A robust and high-throughput Cre reporting and characterization system for the whole mouse brain. Nat Neurosci. 2010; 13:133–140. [PubMed: 20023653]
48. Parslow A, Cardona A, Bryson-Richardson RJ. Sample Drift Correction Following 4D Confocal Time-lapse Imaging. JoVE J Vis Exp. 2014; :e51086–e51086. DOI: 10.3791/51086
49. Longair MH, Baker DA, Armstrong JD. Simple Neurite Tracer: open source software for reconstruction, visualization and analysis of neuronal processes. Bioinformatics. 2011; 27:2453–2454. [PubMed: 21727141]
50. Koudelka S, et al. Individual Neuronal Subtypes Exhibit Diversity in CNS Myelination Mediated by Synaptic Vesicle Release. Curr Biol. 2016; 26:1447–1455. [PubMed: 27161502]

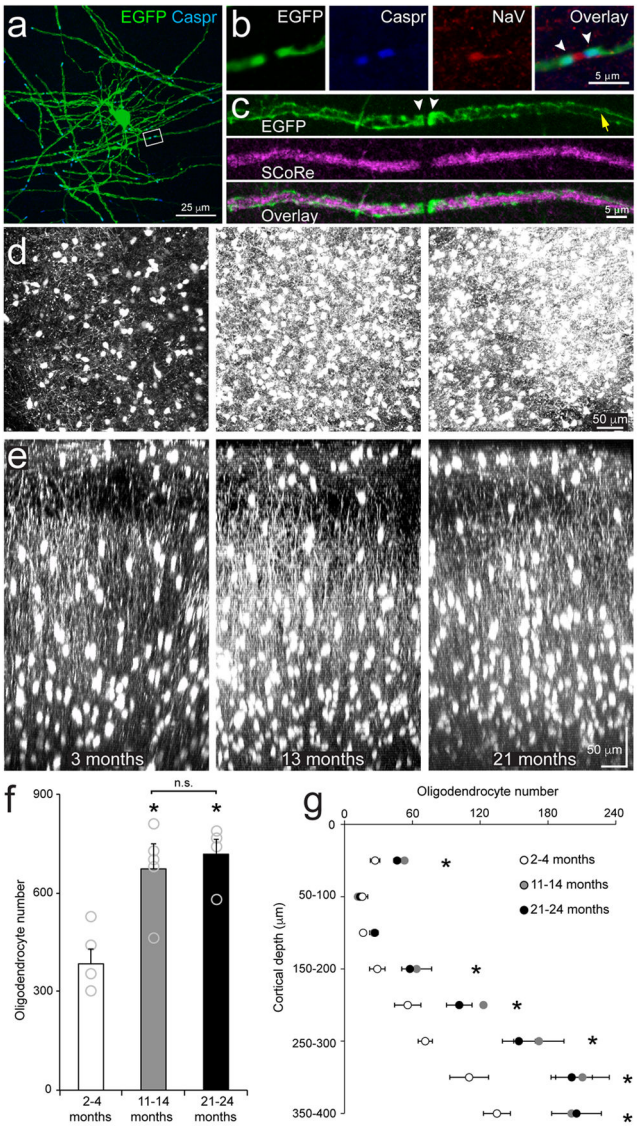

Figure 1. Oligodendrocyte density in upper cortical layers increases during adulthood

a, Maximum projection of an example individual *Mobp-EGFP* oligodendrocyte from a horizontal section (0–50 µm from the pial surface, n = 5 mice) immunolabeled with EGFP and Caspr. **b**, High magnification area from **a**. Putative EGFP+ paranodes (white arrowheads) are immunolabeled with paranodal protein, Caspr, and are adjacent clustered voltage-gated sodium channels (NaV) indicating this is a node of Ranvier. **c**, Maximum projection of a putative EGFP+ myelin sheath in a horizontal section (0–50 µm from the pial surface) immunolabeled with EGFP and imaged with SCoRe. Note the accumulation of EGFP within paranodes (white arrowheads) which lack SCoRe signal. EGFP is also present in cytoplasmic channels (yellow arrow) along the sheath which has strong SCoRe signal indicative of compact myelin. **d**, Maximal Z projection of 400 µm of somatosensory cortex (P90, left; P395, middle; P630, left; *Mobp-EGFP* mouse, (n = 5 mice); chronic cranial window preparation; depth = 0 – 400 µm). **e**, Maximal Y projection of 200 µm of somatosensory cortex (P90, left; P395, middle; P630, left; *Mobp-EGFP* mice; chronic

cranial window preparation). Note high density of oligodendrocytes in Layer I. **f**, Quantification of oligodendrocyte density in layers I–IV (0–400 μm) of somatosensory cortex (2–4 months, n = 5 mice; 11–14 months, n = 6 mice; 21–24 months, n = 4 mice; one-way ANOVA with Tukey post hoc test, 2–4 months vs. 11–14 months, $p = 0.0001$, $q(13) = 9.14$; 2–4 months vs. 21–24 months, $p = 0.0002$, $q(13) = 8.49$; 11–14 months vs. 21–24 months, $p = 0.99$, $q(13) = 0.12$; n.s. = not significant, * = $p < 0.0005$). **g**, Quantification of total oligodendrocyte number in layers I–IV of somatosensory cortex (2–4 months, n = 5 mice; 11–14 months, n = 6 mice; 21–24 months, n = 4 mice; $p<0.05$, one-way ANOVA with Tukey post hoc test, for details see Supplementary Methods Checklist, * = $p < 0.05$). **f,g,** Data are presented as mean ± SEM.

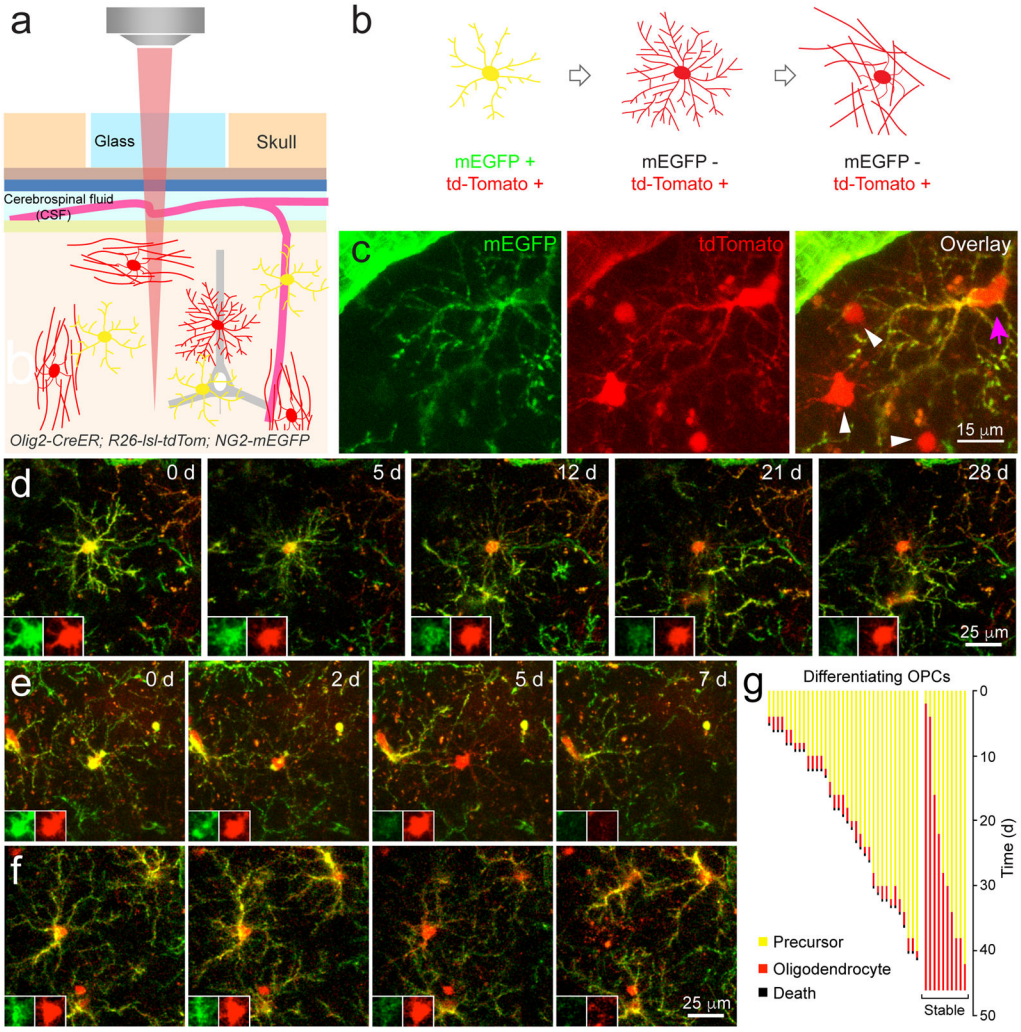

Figure 2. Inefficient integration of newly generated oligodendrocytes in the mature cortex

a, *In vivo* two photon microscopy through chronic cranial windows in *Olig2-CreER; R26-lsl-tdTomato; NG2-mEGFP* triple transgenic mice. **b**, Membrane-anchored EGFP is expressed by OPCs, and all stages of the oligodendrocyte lineage (progenitors, pre-myelinating cells, and mature oligodendrocytes) express tdTomato following administration of tamoxifen. When OPCs differentiate the NG2 promoter is down-regulated and EGFP is no longer expressed, while tdTomato is preserved. **c**, Maximal projection of mEGFP and tdTomato expression in a triple transgenic mouse (P150; depth= 10–19 µm; 100 mg/kg tamoxifen injected for five days at P30; n = 5 mice). OPCs (magenta arrow) express both fluorophores but mature oligodendrocytes only express tdTomato (white arrowheads). Note pericyte expression of mEGFP. **d**, Maximal intensity projection images of a differentiating OPC that becomes a stably integrated oligodendrocyte (P240; depth = 111–120 µm). Images were acquired every 2–3 days for 28 days and relative date of collection is shown in days (d) on each panel. Inset panels show the cell soma at higher magnification for each fluorescent channel. **e**,**f**, Maximal intensity projection images of differentiating OPCs located 234–252 µm (**e**) and 27–61 µm (**f**) below the pial surface (P240). Images were acquired every 2–3

days for one week. Note the fragmentation of the cell in the 7d time point in **f. g**, Quantification of maturation of differentiating OPCs over 1.5 months in P240–426 mice. (n = 3 mice, two imaging volumes/animal; mature oligodendrocytes = 10/45).

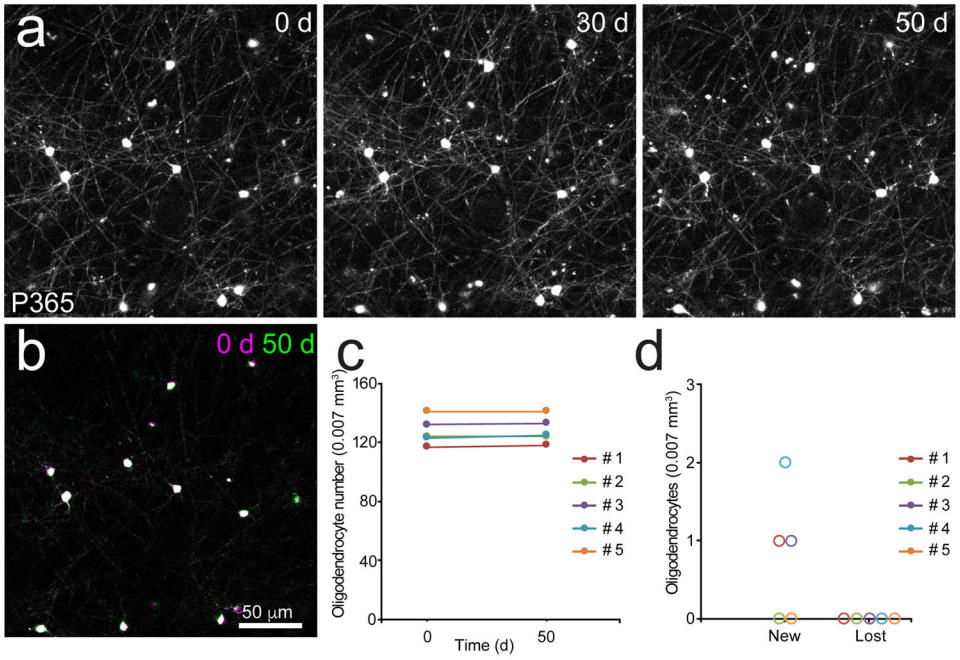

Figure 3. Oligodendrocytes are highly stable in the adult cortex

a, Maximal intensity projection images of oligodendrocytes in the somatosensory cortex of a *Mobp-EGFP* mouse (P365; depth= 45–50 µm). Images were acquired weekly for 50 days. **b**, Montage of 0 (magenta) and 50 (green) day time points. Oligodendrocyte cell body position remains unchanged. **c**, Quantification of oligodendrocyte number over 50 days in >P365 mice. (n = 5 mice; cells = 641). **d**, Quantification of new or lost oligodendrocytes over 50 days in >P365 mice (n = 5 mice).

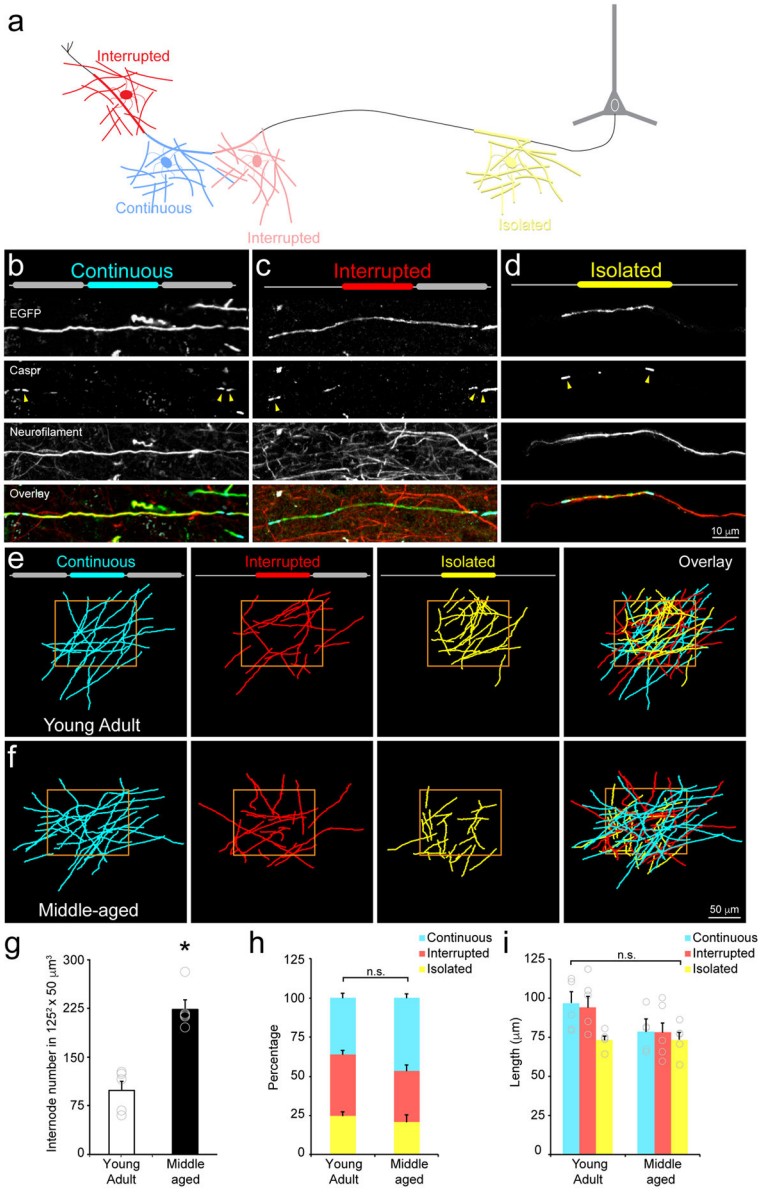

Figure 4. Discontinuous myelination persists in the adult brain

a, Schematic of myelin sheath categorization by the presence or absence of a neighboring sheaths. **b**, Maximum projection of a Continuous myelin sheath. Note doublets of Caspr immunolabeling at both ends of the sheath (yellow arrowheads). **c**, Maximum projection of a Interrupted myelin sheath. Note a doublet of Caspr immunolabeling at one end of the sheath (yellow arrowheads) and the axon extends beyond the Caspr singlet. **d**, Maximum projection of an Isolated myelin sheath. Note only singlets of Caspr immunolabeling at the ends of the sheath (yellow arrowheads) and that the axon extends beyond ends of the sheath. **e**, Projection of traces of EGFP+ myelin internodes within a $125^2 \times 50\ \mu m^3$ area in the somatosensory cortex of a *Mobp-EGFP* mouse (P90; depth = 0–50 μm; n = 5 mice). The position of neighboring internodes on the same axon was used to characterize internodes as Continuous, Interrupted, or Isolated (configuration illustrated by diagram at top of each

panel). **f**, Projection of traces of EGFP+ myelin internodes within 125 μm^2 area in the somatosensory cortex of a *Mobp-EGFP* mouse (P365; depth= 0–50 μm). **g–i**, Quantification of internode number within a $125^2 \times 50$ μm^3 area (**g,** Young Adult: n = 5 mice; Middle-aged: n = 5 mice, p>0.0005, t(8) = −6.02, two-tailed Student's t-test; * = p < 0.0005) and proportion (**h,** Young Adult: n = 5 mice; Middle-aged: n = 5 mice, Continuous, p = 0.17, t(8) = −1.52, Interrupted, p = 0.08, t(8) = 1.98, Isolated, p = 0.53, t(8) = 0.65, two-tailed Student's t-test) and length of each internode class (**i**, Young Adult: n = 5 mice; Middle-aged: n = 5 mice, Continuous, p = 0.13, t(8) = −1.68, Interrupted, p = 0.12, t(8) = −1.72, Isolated, p = 0.97, t(8) = −0.04, two-tailed Student's t-test) for oligodendrocytes within layer I of somatosensory cortex n.s.= not significant. **g–i,** Data are presented as mean ± SEM.

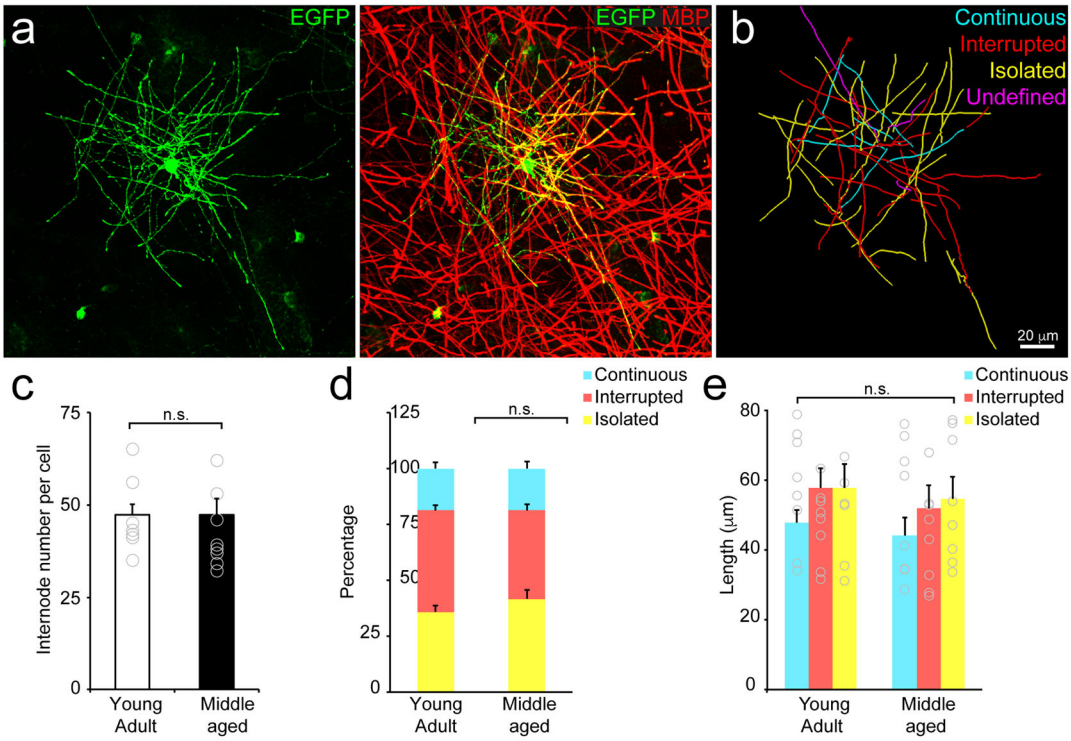

Figure 5. Individual oligodendrocytes generate both Continuous and Isolated internodes

a, Maximum projection an oligodendrocyte (labeled with AAV9-MBP-EGFP) (Left) immunostained with an antibody against MBP (Right). (P90; depth= 50–100 µm). **b,** Traces of EGFP+ myelin internodes of the oligodendrocyte shown in (**a**). Each internode was classified as Continuous, Interrupted, Isolated, or undefined (projects out of tissue section). Quantification of internode number (**c,** Young Adult: n = 5 mice, 8 cells; Middle-aged: n = 5 mice, 8 cells, p = 0.62, t(14) = 0.51, two-tailed Student's t-test) and proportion (**d**, Young Adult: n = 5 mice, 8 cells; Middle-aged: n = 5 mice, 8 cells, Continuous, p = 0.99, t(14) = −0.005, Interrupted, p = 0.11, t(14) = 1.70, Isolated, p = 0.27, t(14) = −1.15, two-tailed Student's t-test) and length of each internode class (**e**, Young Adult: n = 5 mice, 8 cells; Middle-aged: n = 5 mice, 8 cells, Continuous, p = 0.59, t(14) = 0.55, Interrupted, p = 0.52, t(14) = 0.65, Isolated, p = 0.73, t(14) = 0.36, two-tailed Student's t-test, n.s. = not significant) for individual oligodendrocytes within layer I of cortex. **c-e,** Data are presented as mean ± SEM.

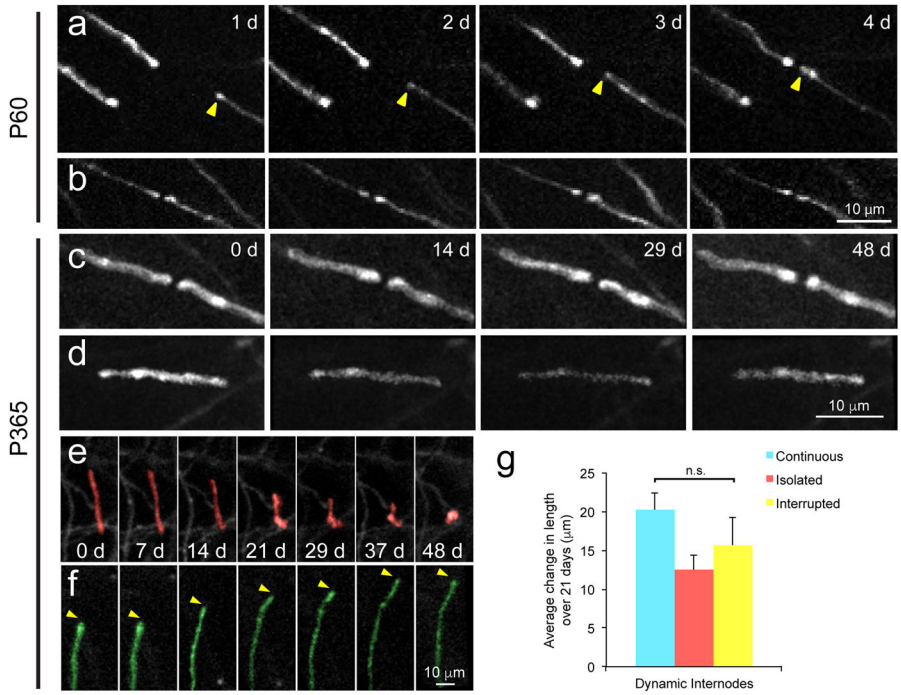

Figure 6. Infrequent remodeling of myelin internodes in the somatosensory cortex

a, *In vivo* time lapse images of oligodendrocyte processes in *Mobp-EGFP* mice (n = 5 mice). An extending process of a newly generated oligodendrocyte (yellow arrowhead) that forms a new node of Ranvier. **b**, An existing node exhibits little change in structure over four days (P60; depth= 24–27 μm; thinned-skull preparation, n = 5 mice).) **c,d**, Maximal intensity projection image of Continuous internodes (P365; depth= 39–43 μm) (**c**) and an isolated internode (P365; depth= 31–35 μm) (**d**) that remain unchanged over 48 days. **e,** Maximal intensity projection images illustrating retraction of an internode (red; P365; depth= 63–67 μm). **f**, Maximal intensity projection image illustrating extension of an internode (green; P365; depth= 63–67 μm). No newly generated or dying oligodendrocytes were found within 250 μm of these internodes. **g**, Quantification of the average change in length of dynamic internodes over three weeks in P365 mice. (n= 20 mice, p = 0.62, F(3, 35) = 0.49, one-way ANOVA, n.s.= not significant; mean ± SEM).

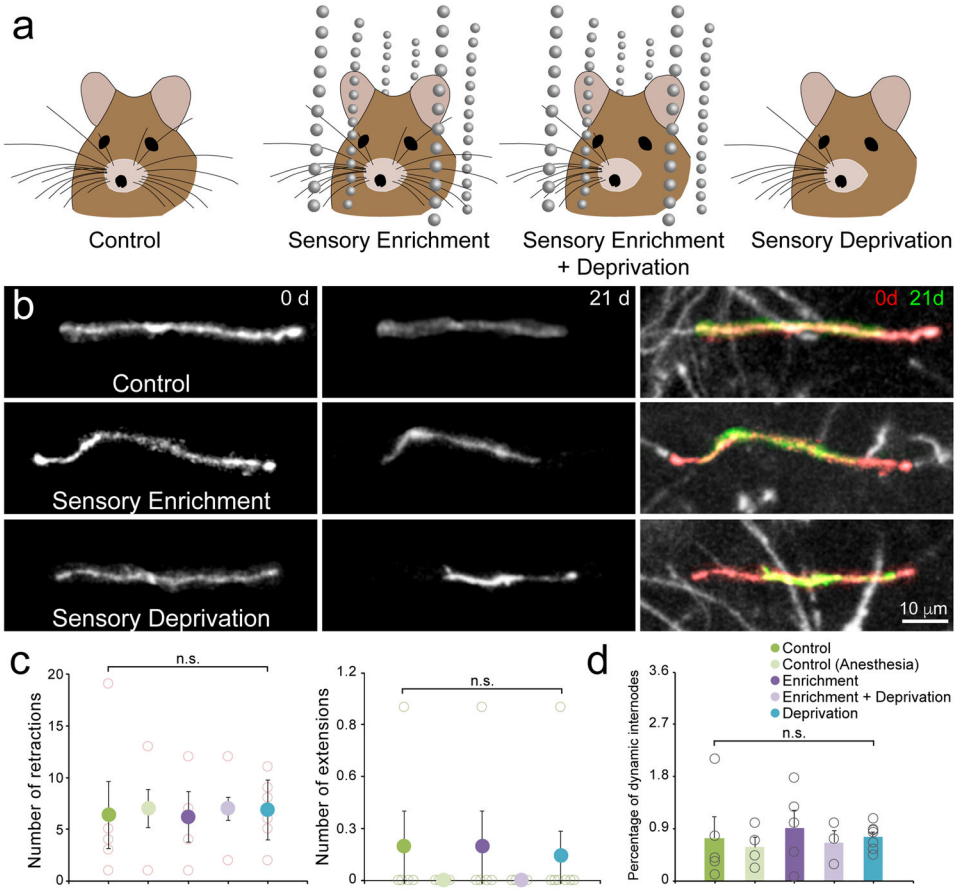

Figure 7. Sensory enrichment does not influence myelin remodeling in middle-aged animals

a, Illustration of different configurations to test role of sensory enrichment on myelin dynamics. Mice are housed in cages with or without sensory enrichment (hanging beads), or with or without left-sided whiskers for 21 days. **b**, Maximal intensity projection images of internodes imaged in the right somatosensory barrel cortex (top, P365; depth= 150–159 µm; middle, P365; depth= 183–192 µm; bottom, P365; depth= 210–232 µm) that decrease in length over 21 days. Red areas in Overlay highlight extent of retraction. **c**, Quantification of internode retraction (left) and extension (right) over 21 days in P365 mice in a 425 μm^2 × 100 µm area. Individual mouse values: open circles; Mean value: filled circles. (Control, n = 6 mice; Control (Anesthesia), n = 4 mice; Enrichment, n = 5; Enrichment + Deprivation, n = 3 mice; Deprivation, n = 7 mice; retractions p = 0.99, F(4,19) = 0.03, extensions p = 0.86, F(4,19) = 0.32, One-way ANOVA). **d**, Quantification of percentage of total internodes that were dynamic over 21 days in P365 mice in a 425 μm^2 × 100 µm area. Individual mouse values: open circles; Mean value: filled circles. (Control, n = 6 mice; Control (Anesthesia), n = 4 mice; Enrichment, n = 5; Enrichment + Deprivation, n = 3 mice; Deprivation, n = 7 mice; p = 0.91, F(4,19) = 0.25, One-way ANOVA; n.s. = not significant). **c–d,** Data are presented as mean ± SEM.

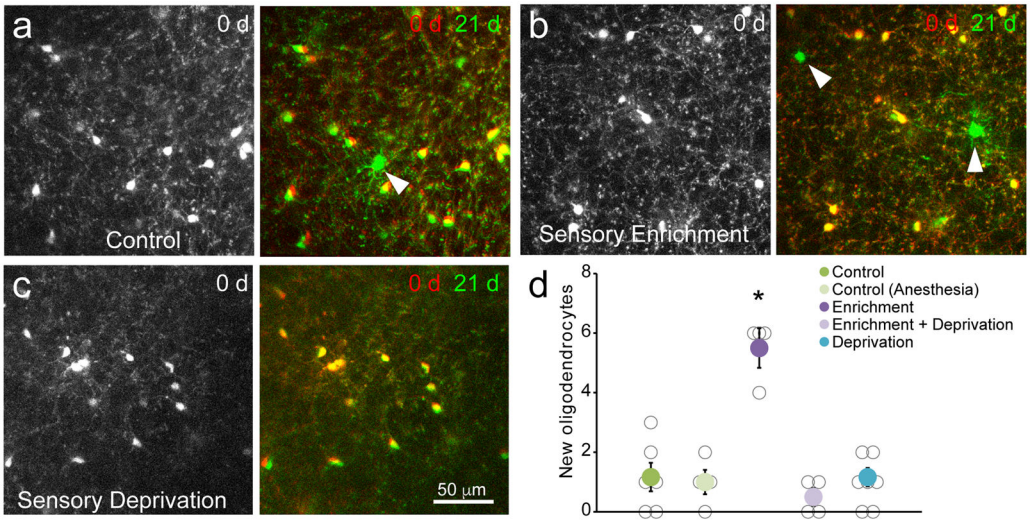

Figure 8. Sensory enrichment increases oligodendrogenesis in middle-aged animals

a–c, *In vivo* imaging of oligodendrocytes in the somatosensory cortex of *Mobp-EGFP* mice (P365; depth= 300–312 μm) showing the density of oligodendrocytes in one imaging field on day 0 (Left) and an overlay of the same field on day 0 and day 21 (Right). Control mouse in standard housing (**a**), mouse housed with sensory enrichment (**b**), and mouse in standard housing without whiskers (**c**). New oligodendrocytes are marked with white arrowheads. **d**, Quantification of oligodendrocyte addition over three weeks in P365 mice in a 425 μm^2 × 400 μm area. (Control, n = 6 mice; Control (Anesthesia), n=4 mice; Enrichment, n = 4; Enrichment + Deprivation, n = 4 mice; Deprivation, n = 7 mice; * = $p < 0.001$, One-way ANOVA with Tukey's posthoc test; mean ± SEM).